Developmental Cell
Article

Angiogenic Sprouting Requires the Fine Tuning of Endothelial Cell Cohesion by the Raf-1/Rok-α Complex

Reiner Wimmer,[1] Botond Cseh,[1] Barbara Maier,[1] Karina Scherrer,[1] and Manuela Baccarini[1,*]
[1]Department of Microbiology and Immunobiology, University of Vienna, Max F. Perutz Laboratories, Doktor-Bohr-Gasse 9, 1030 Vienna, Austria
*Correspondence: manuela.baccarini@univie.ac.at
DOI 10.1016/j.devcel.2011.11.012

SUMMARY

Sprouting angiogenesis, crucial for the development of new blood vessels, is a prime example of collective migration in which endothelial cells migrate as a group joined via cadherin-containing adherens junctions (AJ). The actomyosin apparatus is connected to AJ and generates contractile forces, which, depending on their strength and duration, increase or decrease cell cohesion. Thus, appropriate spatiotemporal control of junctional myosin is critical, but the mechanisms underlying it are incompletely understood. We show that Raf-1 is an essential component of this regulatory network and that its ablation impairs endothelial cell cohesion, sprouting, and tumor-induced angiogenesis. Mechanistically, Raf-1 is recruited to VE-cadherin complexes by a mechanism involving the small G protein Rap1 and is required to bring the Rho effector Rok-α to nascent AJs. This Raf-1-mediated fine tuning of Rok-α signaling allows the activation of junctional myosin and the timely maturation of AJ essential for maintaining cell cohesion during sprouting angiogenesis.

INTRODUCTION

Angiogenesis is a complex process involving the migration and proliferation of endothelial cells (ECs) and their incorporation into new blood vessels. During embryonic life, this process is essential for cardiovascular development. In the adult, angiogenesis is crucial for tissue regeneration, for the establishment of chronic inflammatory conditions, and, most notably, for tumor development. Angiogenesis ensures the supply of nutrients and oxygen to the growing tumor, which expresses pro-angiogenic proteins, such as VEGF, FGF-2, TGF-β, and others to recruit vascular ECs from neighboring blood vessels (Chung et al., 2010). During this process, called sprouting angiogenesis, ECs must coordinate two programs: one that allows the emergence of tip cells, which detach from the existing vessels and migrate following guidance cues, providing directionality to the developing vessel network; and a program that supports the growth of the sprout by stabilizing the contacts between the tip and the stalk cells, which form the stem of the developing sprout (Eilken and Adams, 2010). Both programs crucially depend on dynamic changes in cell cohesion and on the remodeling of the cytoskeleton.

In ECs, as well as in epithelial cells, initial cell-cell contacts involve the adherens junctions (AJ), in which adhesion is mediated by homophilic interaction of classical cadherin molecules expressed by neighboring cells (VE-cadherin in endothelial, E-cadherin in epithelial cells). The extracellular cadherin domains initiate contact, whereas the cytoplasmic tails bind to proteins that anchor the junctions to the actin cytoskeleton. The formation of cadherin clusters and their interaction with the cytoskeleton, particularly with the actomyosin contractile apparatus, allow the maturation of the cell-cell contacts; at the same time, the connection with actomyosin allows the junctions to sense and respond to mechanical stress (Dejana et al., 2009; Liu et al., 2010; Papusheva and Heisenberg, 2010). The small GTPases Rap, Rac, and Rho regulate AJ dynamics during the formation of both epithelial and endothelial cell-cell contacts (Cascone et al., 2003; Dejana et al., 2009; Kooistra et al., 2007; Liu et al., 2010; Pannekoek et al., 2009; Yamada and Nelson, 2007); however, the precise molecular mechanisms mediating the generation and spatial control of contractile forces at the AJ are not yet understood completely.

In ECs, cell-cell contact and VE-cadherin (VEC) antagonize angiogenic sprouting by restraining VEGF-induced proliferation (Grazia Lampugnani et al., 2003; Lampugnani et al., 2006); VEGF, in turn, might counteract cell-cell contact formation by inducing VEC endocytosis (Gavard and Gutkind, 2006). In addition, VEC restrains tubulogenesis and sprout formation in zebrafish and in three-dimensional (3D) human umbilical vein endothelial cells (HUVECs) cultures through a mechanism involving the phosphorylation of myosin light chain 2 (MLC2) mediated by the Rho effector kinase Rok (Abraham et al., 2009). Rok activity and phosphorylation of cortical MLC limit the protrusional activity of tip cells and branching (Fischer et al., 2009); on the other hand, Rho activity is necessary for the assembly of ECs in new vessels in vivo (Hoang et al., 2004). Thus, a tight control of Rho downstream pathways is crucial for successful angiogenesis.

Raf-1, a member of the Raf family of protein kinases (A-Raf, B-Raf, and Raf-1, also known as C-Raf) linking Ras activation to the ERK pathway, has been previously implicated in angiogenesis. In ECs, activation of Raf-1 by VEGFA and FGF-2

promotes survival in an ERK-dependent or independent manner, respectively (Alavi et al., 2003; Alavi et al., 2007; Hood et al., 2002). In the past few years, gene ablation studies have highlighted other ERK-independent essential functions of Raf-1, such as promoting migration and protecting cells from apoptosis (Ehrenreiter et al., 2005; Mikula et al., 2001; Piazzolla et al., 2005). These functions do not require Raf-1 kinase activity and are based on Raf-1's ability to interact with, and inhibit, the proapoptotic kinases ASK-1 and MST2, as well as Rok-α (Baccarini, 2005; Niault et al., 2009). The Raf-1/Rok-α interaction is also essential for the development and maintenance of Ras-driven epidermal tumors (Ehrenreiter et al., 2009).

Here, we show that Raf-1 is required for the establishment of tumor-associated vasculature in vivo and for sprouting in 3D EC cultures. In Raf-1-deficient ECs, the formation of AJ and their coupling to actomyosin contractility is delayed; mechanistically, Raf-1 is recruited to VEC-containing AJ by a mechanism involving the small G protein Rap1, and this step is required for the localization of the Rok-α to the AJ and for the timely phosphorylation of MLC2 in these structures. These data demonstrate a crucial role of the Raf-1/Rok-α complex in the generation of spatially controlled actomyosin activity during the formation of VEC-containing AJ.

RESULTS

Raf-1 Is Required for Sprouting of Primary ECs in 3D Cultures and for Pathological Angiogenesis In Vivo

Ablation of the *c-raf-1* gene in ECs was achieved by combining the Tie2-Cre transgene (Forde et al., 2002) with a homozygous *c-raf-1*$^{f/f}$ allele (Jesenberger et al., 2001). These mice (*c-raf-1*$^{\Delta/\Delta EC}$, deleted in ECs) were born at mendelian ratios (see Supplemental Experimental Procedures available online) and exhibited a normal life span. Raf-1 ablation was confirmed by the analysis of primary microvessel-derived mouse ECs (pMECs) isolated from the lung of Raf-1$^{\Delta/\Delta EC}$ animals, which showed complete conversion of the *c-raf-1*^{flox} to the *c-raf-1*$^{\Delta}$ allele by PCR and did not express the Raf-1 protein (see Supplemental Experimental Procedures). The blood vessel structure and tissue architecture of Raf-1$^{\Delta/\Delta EC}$ and f/f kidneys, lungs, and livers was indistinguishable (Figure S1A). In contrast, analysis of the developing retinal vasculature on postnatal day 6 revealed a delay in the progression of the angiogenic front toward the periphery (Figure S1B). Branching was also compromised (Figure S1C), and the Raf-1$^{\Delta/\Delta EC}$ angiogenic front contained increased numbers of tip cells extending filopodia and thus acquiring a motile, exploratory phenotype (Figure S1D). Mitotic and apoptotic indexes were comparable in the f/f and Raf-1$^{\Delta/\Delta EC}$ retinas, and the knockout did not influence vessel stability (data not shown). Together, the data suggest that Raf-1 ablation impacts collective, but not single cell migration in vivo. Consistent with these in vivo data, Raf-1$^{\Delta/\Delta}$ EC migrated slightly faster than f/f cells in a transwell assay (Figure S1F), proliferated normally, and did not show increased apoptosis (data not shown) in conventional two-dimensional (2D) culture systems. In addition, ERK phosphorylation levels were similar or higher in continuously growing or FGF-2-stimulated Raf-1$^{\Delta/\Delta}$ ECs than in f/f ECs (Figures S1G and S2G). In contrast to this inconspicuous behavior in 2D cultures, Raf-1$^{\Delta/\Delta}$ pMECs showed severe defects in angiogenesis assays in 3D cultures. Aorta explants from Raf-1$^{\Delta/\Delta EC}$ mice showed dramatically reduced sprouting into fibrin gels (Figure S2A). Yet more compelling were the results obtained by testing the ability of pMECs cultured on microcarrier beads to form sprouts in fibrin gels, an assay that recapitulates the salient steps of sprouting: migration, proliferation, alignment, and tube formation (Nakatsu et al., 2007) (Figure S2B). While f/f pMECs migrated out of the beads and formed complex tubular networks within 3 days, the number and length of sprouts formed by Raf-1$^{\Delta/\Delta}$ was dramatically reduced (Figure 1A). Importantly, Raf-1$^{\Delta/\Delta}$ pMECs adhered to the microcarrier and proliferated as efficiently as f/f pMECs (Figures S2C and S2D). They were able to assume a mesenchymal morphology, reminiscent of the excess tip cells observed in the developing retina, and to efficiently migrate out of the beads (Figures 1B and 1C; Figure S2E). Video microscopy revealed that f/f cells aligned and remained connected during sprout formation. In Raf-1$^{\Delta/\Delta}$ pMEC cultures, in contrast, the tip cells broke off from the developing tubule, migrating further in the fibrin gel, and finally undergoing membrane blebbing and apoptosis (Figure 1B; Movies S1 and S2).

To determine whether these sprouting defects had a counterpart in the adult animal, we investigated neovascularization by subcutaneously injecting f/f and Raf-1$^{\Delta/\Delta EC}$ mice with FGF-2/VEGF-supplemented matrigel. The numbers of proliferating and apoptotic ECs in plugs isolated from control and Raf-1$^{\Delta/\Delta EC}$ mice 10 days after injection were similar (Figures S2F and S2G); however, plugs harvested from Raf-1$^{\Delta/\Delta EC}$ mice were much less vascularized (Figures 1D and 1E), and the few vessels were restricted to the edges of the plug (Figure 1D). In addition, subcutaneously grafted Lewis lung carcinoma (LLC-1) cells grew poorly in Raf-1$^{\Delta/\Delta EC}$ mice, and the vascular density in the grafts was greatly reduced (Figures 1F and 1G). Thus, the presence of Raf-1 in ECs is necessary for pathological angiogenesis.

Raf-1 Is Required for the Establishment of VEC-Containing AJ

The sprouting phenotype of Raf-1$^{\Delta/\Delta}$ pMECs was consistent with a defect in cell-cell adhesion, which depends on VEC (Abraham et al., 2009). VEC expression (Figure 2A) and membrane localization (see Supplemental Experimental Procedures) were similar in confluent 2D f/f and Raf-1$^{\Delta/\Delta}$ MECs monolayers. In 3D cultures, however, VE-cadherin was diffusely localized in Raf-1$^{\Delta/\Delta}$ pMECs, even in those forming sprouts, in contrast to flox/flox cells, in which this molecule was clearly concentrated in AJ (Figure 2B). VE-cadherin mislocalization could also be observed in vivo, in the Raf-1$^{\Delta/\Delta EC}$ sprouts invading matrigel plugs (Figure 2C), and in the tip cells of Raf-1$^{\Delta/\Delta EC}$ retinas (Figure S1E).

Analysis of AJ formation after replating in 2D cultures showed that VEC-containing junctions appeared, spread, and matured with considerable delay in immortalized Raf-1$^{\Delta/\Delta}$ EC cultures (iMECs; Figure 2D). Active myosin II, which mediates VEC localization to cell-cell junctions and connects these structures to the actomyosin system (Abraham et al., 2009), was detected as phosphorylated MLC2 (pMLC2) in cell-cell contacts of f/f iMECs. In contrast, less pMLC2 could be detected in the AJ developing between Raf-1$^{\Delta/\Delta}$ MECs (Figure 2D), although the total amount of pMLC2 was slightly increased in these cells (Figure 2A). As in HUVECs (Abraham et al., 2009), treatment with an

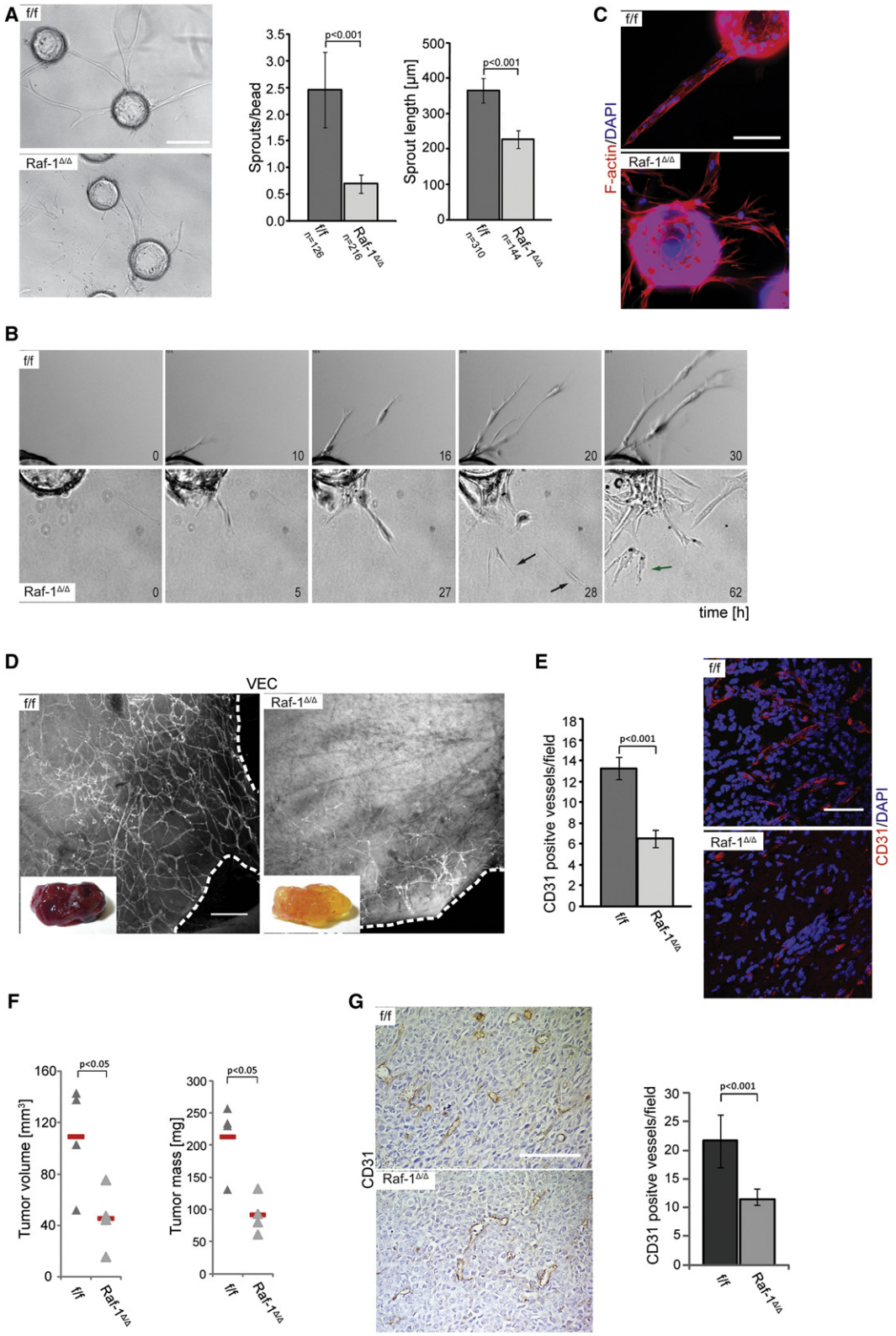

Figure 1. Raf-1 Is Required for In Vitro Sprouting in 3D Fibrin Gels and In Vivo for Pathological Angiogenesis

(A) pMECs isolated from Raf-1$^{\Delta/\Delta EC}$ animals show dramatically reduced sprouting in 3D fibrin gels. pMECs were allowed to adhere to microcarriers and embedded in fibrin gels containing FGF-2 and VEGF (200 ng/ml each). The number of sprouts/bead and the length of sprouts were microscopically assessed after 3 days in culture. The results are plotted in the right panel. n = number of microcarriers evaluated; error bars, SD of the mean.

inhibitor of Rho-dependent kinases (Rok; Y-27632) abrogated junctional actomyosin activation (Figure 2D). In 3D pMEC cultures, 10 μM of Y-27632 increased sprouting of control cells (Abraham et al., 2009), but higher concentrations of the inhibitor dramatically decreased it, phenocopying the sprouting defect of Raf-1$^{\Delta/\Delta}$ pMECs (Figure 2E).

Raf-1 Is Required for the Recruitment of Rok-α to AJ

Raf-1 interacts with, and regulates, the MLC2 activator Rok-α (Ehrenreiter et al., 2009; Ehrenreiter et al., 2005; Niault et al., 2009; Piazzolla et al., 2005). Thus, a defect in Rok-α localization or activity could underlie the diffused VEC staining and the lack of pMLC2 observed in the developing Raf-1$^{\Delta/\Delta}$ AJ. As in other cell types (Ehrenreiter et al., 2009; Ehrenreiter et al., 2005; Niault et al., 2009; Piazzolla et al., 2005), lack of Raf-1 in MECs did not alter Rok-α expression, whereas a number of Rok-α downstream targets, with the notable exception of junctional pMLC2, were slightly hyperphosphorylated (Figures 2A and 2D).

To gain insight in the molecular mechanisms underlying the phenotype of Raf-1$^{\Delta/\Delta}$ MECs, we analyzed VEC complexes. Unexpectedly, VEC immunoprecipitates from f/f cells contained low amounts of Raf-1, which reproducibly increased upon stimulation of iMECs with VEGF (not significant) and FGF-2 (Figures 3A and 3B). Rok-α was recruited to VEC with kinetics similar to Raf-1 (Figures 3B–3D). The fraction of Raf-1 and Rok-α binding to VEC was higher in confluent than in sparse cultures, implying that AJ are required for the interaction (Figure 3C). In Raf-1$^{\Delta/\Delta}$ iMECs, however, the FGF-2- and VEGF-mediated recruitment of Rok-α to VEC was abrogated, whereas the recruitment of β and p120 catenins was unperturbed (Figure 3D). Thus, Raf-1 is selectively required for efficient growth factor-mediated recruitment of Rok-α to AJ. Consistently, FGF-2 induced phosphorylation of the Rok downstream effector MLC2 in both f/f and Raf-1$^{\Delta/\Delta}$ iMECs, but in the latter cells, pMLC failed to localize to the cell-cell contacts (Figure 3E). The appearance of junctional pMLC2 correlated with the colocalization of Rok-α with VEC at cell-cell contacts (Figure 3F), also selectively lost in Raf-1$^{\Delta/\Delta}$ MECs. Rok-β, in contrast, did not coimmunoprecipitate with VEC or Raf-1 and did not colocalize with VEC at AJ (Figures S3A and S3B).

Importantly, loss of junctional pMLC could also be observed in the short vessels invading the matrigel plugs implanted in Raf-1$^{\Delta/\Delta EC}$ mice (Figure 3G). This is consistent with the mislocalization of VEC observed in Raf-1$^{\Delta/\Delta EC}$ sprouts (Figure 2C) and indicates that the molecular phenotype induced by Raf-1 ablation is the same in vivo and in culture. Collectively, the results show that Raf-1 is essential for bringing Rok-α to developing VEC-containing cell-cell contacts. Rok-α in turn mediates the phosphorylation of MLC2 at the AJ, where it is required for the homogeneous distribution of VEC at the cell-cell junctions and for the stabilization of sprouts.

The Regulatory N-Terminal Domain of Raf-1 Is Sufficient to Rescue the Sprouting Defects

To further explore the function of Raf-1 in sprouting, we transfected Raf-1$^{\Delta/\Delta}$ pMECs with vectors expressing Raf-1 proteins fused to GFP. Fluorescence-activated cell-sorted GFP-expressing cells were used in a 3D sprouting assay. Vector-transfected clones (eV) performed as poorly as Raf-1$^{\Delta/\Delta}$ pMECs in the sprouting assay, whereas full-length kinase-competent or kinase-dead Raf-1 fully rescued sprouting (Figure 4A) and VEC localization to AJ (Figure 4C). The Raf-1 N-terminal regulatory domain (NT) also restored sprouting and VEC distribution to wild-type levels (Figures 4A and 4B). N-terminal regulatory domain contains an element essential for Raf-1 activation and membrane recruitment by small G proteins, such as Ras (Ras binding domain [RBD]); and a Cystein-rich domain (CRD), which is essential for auto-inhibition and for the interaction with Rok-α (Niault et al., 2009). A mutation that compromises Rok-α binding (CC165/168SS; NT CC/SS) failed to rescue sprouting and VEC delocalization of the Raf-1$^{\Delta/\Delta}$ ECs (Figure 4B). Thus, the ability of Raf-1 to bind to Rok-α, but not Raf-1 kinase activity, is required for efficient sprouting and cell-cell adhesion. A second Raf-1 mutant (R89L; NT R89L), capable of binding to Rok-α, but not to Ras (Niault et al., 2009) or Rap1 (Herrmann et al., 1996; Nassar et al., 1996; Nassar et al., 1995), was similarly ineffective in rescuing the phenotypes (Figures 4B and 4C), suggesting that G protein binding was essential for the localization of the Raf-1/Rok-α complex to VEC-containing junctions.

EPAC Activation Recruits the Raf-1/Rok-α Complex to VEC-Containing Junctions

Ras is not reported to localize to AJ, and its activation does not promote AJ formation but rather induces their disassembly to increase cell motility (Popoff and Geny, 2009). In contrast, Rap1 is present in VEC-containing junctions (Dejana et al., 2009) and has been implicated in the formation and tightening of AJ in both ECs and epithelial cells (Kooistra et al., 2007; Pannekoek et al., 2009) and in sprouting downstream of FGF (Yan et al., 2008). Intriguingly, the phenotypes of Raf-1 and Rap1 knockout ECs partially overlap (Carmona et al., 2009; Chrzanowska-Wodnicka et al., 2008; Yan et al., 2008).

(B) Sprout formation monitored by time lapse microscopy. Still images taken at different time points during sprouting are shown. In Raf-1$^{\Delta/\Delta}$, pMEC cultures single-tip cells break off from the developing sprouts, migrate as single cells (black arrow), and eventually undergo apoptosis, as indicated by membrane blebbing (green arrow).

(C) Raf-1$^{\Delta/\Delta}$ pMECs exhibit a mesenchymal phenotype during sprouting in fibrin gels. Cultures were stained with Rhodamin-phalloidin to visualize F-actin structures.

(D and E) Raf-1$^{\Delta/\Delta EC}$ mice fail to vascularize subcutaneous matrigel plugs. Matrigel, containing FGF-2 and VEGF (1 μg each), was subcutaneously injected into f/f and Raf-1$^{\Delta/\Delta EC}$ mice. Ten days later, plugs were fixed and stained with anti-VEC antibodies (D) or with CD31/DAPI to visualize ECs. In (D), dashed lines indicate the outer margin of the plug. In (E), a quantification of CD31-positive vessels/field is shown in the right panel. Four plugs/genotype were analyzed; error bars, SD of the mean.

(F and G) Raf-1 ablation impairs xenograft growth and vascularization. The graph shows tumor volume and mass assessed 14 days after subcutaneous implantation of 10^6 Lewis lung carcinoma cells (LLC-1) into f/f and Raf-1$^{\Delta/\Delta EC}$ mice. In (G), CD31 immunohistochemistry was used to visualize ECs and vessels invading the tumors. A quantification of the CD31-positive vessels/field is shown in the right panel; error bars, SD of the mean. Scale bars: (A), (D), and (E), 200 μm; (C) and (G), 100 μm. p values are according to Student's t tests. See also Figures S1 and S2 and Movies S1 and S2.

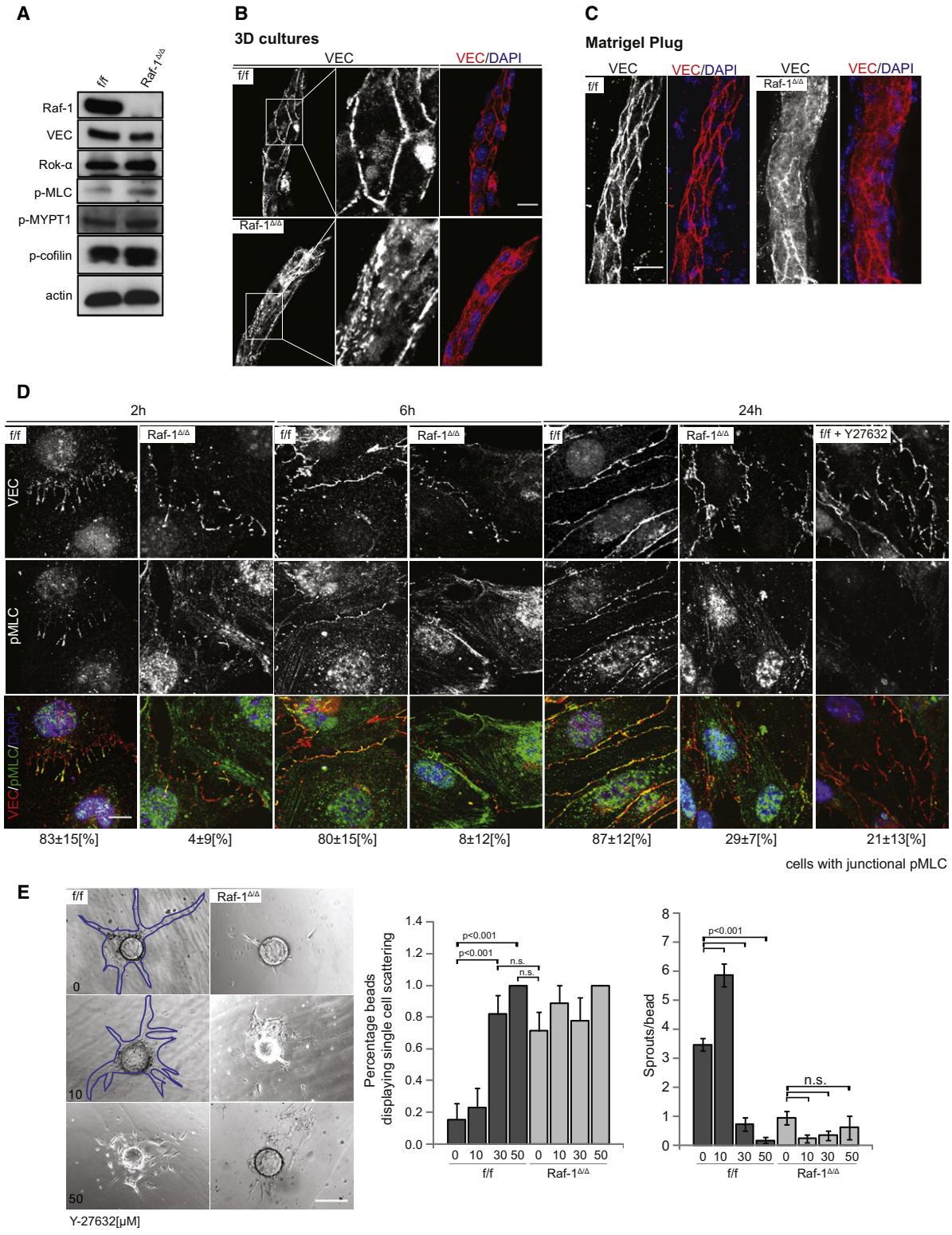

Figure 2. Raf-1 Affects VEC-Mediated AJ Formation

(A) Rok-α substrates are slightly hyperphosphorylated in continuously growing Raf-1$^{\Delta/\Delta}$ pMECs. Expression of Raf-1, VEC, and Rok-α, and phosphorylation of Rok-α downstream targets were detected by immunoblotting.

(B and C) VEC fails to localize at cell-cell borders in sprouts formed by Raf-1$^{\Delta/\Delta}$ pMECs in 3D cultures (B) and in matrigel plugs (C). VEC patterns (red) and nuclei (DAPI, blue) were analyzed by confocal microscopy.

In ECs, Rap1-induced tightening of AJ (Kooistra et al., 2005) and VEC stabilization at the cell-cell contacts (Noda et al., 2010) depend on the cAMP-inducible Rap1 GEF (guanine-nucleotide exchange factor) EPAC. As previously reported (Wittchen et al., 2005), the cAMP analog 007 [8-(4-chloro-phenylthio)-2′-O-methyladenosine-3′,5′-cyclic monophosphate] (Enserink et al., 2002), a selective EPAC activator, accelerated AJ formation among f/f cells after replating and potently induced the colocalization of VEC and pMLC2 at nascent junctions. Both effects were blunted in Raf-1$^{\Delta/\Delta}$ iMECs (Figure 5A); the lack of junctional myosin activation in Raf-1$^{\Delta/\Delta}$ iMECs correlated with a failure to remodel the actin cytoskeleton and establish the cortical actin band, which stabilizes AJ (Figure 5B). The effects of 007 on AJ maturation and cytoskeletal rearrangements were completely abrogated by a Rok inhibitor, which phenocopied the situation in Raf-1$^{\Delta/\Delta}$ iMECs (Figure 5C). Thus, 007 increased AJ maturation by a mechanism dependent on both Raf-1 and Rok.

Consistent with this, both 007 and FGF-2 induced the association between Raf-1 and VEC (Figures 6A and 6B). Increased complex formation was sensitive to GGTi-298, a potent, selective inhibitor of Rap prenylation (Qian et al., 1998) (Figures 6A and 6B) and to the compound siRNA-mediated knockdown of Rap1A and B (Figure 6C). Consistently, Rap1A/B knockdown (Figure 6D; Figure S4) or Rap inhibition by GGTi-298 (Figure S4) severely impaired AJ maturation and Rok-α localization to developing AJs. Similarly, recruitment of Rok-α to the AJ failed in Raf-1$^{\Delta/\Delta}$ iMECs, indicating that both Rap1 and Raf-1 are essential for this process (Figures 6D and 6E).

FGF-2 and 007 treatment had hardly any effect on the association between Raf-1 and Rok-α, (Figure 6B), suggesting that they were recruited to VEC as a complex. Rok-β could not be found in VEC or Raf-1 immunoprecipitates, and did not colocalize with VEC in f/f cells (Figure S4); consistently, siRNA-mediated knockdown of Rok-α, but not Rok-β, impaired 007-induced AJ maturation in f/f cells (Figure 6F).

DISCUSSION

Rho-dependent myosin contractility has emerged as a central regulator of AJ size and strength. In established AJ, increased contractility correlates with the weakening of the junctions and with increased endothelial permeability (Dudek and Garcia, 2001; Rolfe et al., 2005). During sprouting, myosin activation must be tightly controlled because if it happens too fast or is unduly strong or prolonged, the junctions will not be plastic enough to allow sprouting (Abraham et al., 2009). On the other hand, endogenous tugging forces generated locally by Rho/Rok-dependent myosin activation promote junction growth (Liu et al., 2010); if these forces are not timely generated or they are too weak, the junction's growth and stabilization will be delayed. This dual role of myosin activation in junction plasticity is reflected by the effect of a Rok-inhibitor on sprouting f/f 3D cultures. Partial inhibition of Rok by low concentrations of the inhibitor, which reportedly increase Rac1 activity (Abraham et al., 2009), enhances sprouting; higher concentrations, however, block AJ growth (Liu et al., 2010) and inhibit sprouting (Figure 2E). Similarly, both accelerating and delaying AJ maturation by activating or inhibiting Rap1 suppresses sprouting (Figure S5). The latter treatments phenocopy the defects of ECs lacking Raf-1; in 3D sprouting assays, the most obvious consequence of Raf-1 ablation is the formation of cell-cell contacts that cannot be stabilized fast enough to withstand the pull of the tip cell, which breaks off the developing sprout and eventually dies (Figure 1B; Movies S1 and S2). Thus, in contrast to other cell types and tissues in which Raf-1's main role is that of an endogenous Rok-α inhibitor, and in which chemical or genetic Rok-α inhibition rescues the Raf-1 knock-out phenotypes (Ehrenreiter et al., 2009; Ehrenreiter et al., 2005; Niault et al., 2009; Piazzolla et al., 2005), in ECs Raf-1 is a crucial component of the molecular machinery linking VEC to Rok-α signaling and myosin activation.

Raf-1 modulates myosin activation at VEC-containing contacts by bringing Rok-α to these structures. Both kinases are present in VEC immunoprecipitates from f/f cells treated with agents that modulate AJ formation, but much less Rok-α coprecipitates with VEC in Raf-1$^{\Delta/\Delta}$ iMECs, resulting in a dramatic reduction of activated myosin selectively at AJ (Figures 2, 3, 5, and 6). The hyperphosphorylation of Rok-α downstream targets observed in Raf-1 knock-out MECs (Figure 2A), albeit subtle, suggests that Raf-1 might in addition function as an endogenous Rok-α inhibitor, as described in other cell types (Ehrenreiter et al., 2009; Ehrenreiter et al., 2005; Niault et al., 2009; Piazzolla et al., 2005). On this basis, it is tempting to speculate that Raf-1 might both recruit Rok-α to VEC and dim its activity at the AJ. Such a mechanism would ensure tight regulation of Rok-α signaling at the AJ, preventing excessive actomyosin contractility and the generation of centripetal forces that might ultimately destabilize the AJ. The lack of phenotype in Raf-1$^{\Delta/\Delta}$ MEC monolayers and in unperturbed *c-raf-1*$^{\Delta/\Delta EC}$ adult mice compared with the defects in AJ development, sprouting and neovascularization, indicate that the Raf-1-mediated fine tuning of Rok-α is most important for AJ plasticity in the course of remodeling processes, rather than in the AJ maintenance.

How is the complex recruited to AJ? The N-terminal regulatory domain of Raf-1 is sufficient to rescue the sprouting defects of Raf-1$^{\Delta/\Delta}$ pMECs, but mutation of either the RBD or the CRD,

(D) Delayed formation of VEC-containing AJ and mislocalization of activated myosin (pMLC) in Raf-1$^{\Delta/\Delta}$ iMECs. iMECs were seeded on chamber slides in the presence of FGF-2 (50 ng/ml) and fixed at the indicated time points. The localization of VEC (red) and pMLC (green) was analyzed by confocal microscopy. Nuclei were stained with DAPI (blue). Note the consistent colocalization of VEC and pMLC in the f/f iMECs and the lack of colocalization in the Raf-1$^{\Delta/\Delta}$ cells or in cells treated with the Rok inhibitor (20 μM Y-27632). The numbers below the pictures indicate the percentage of cells positive for junctional pMLC, ± SD.
(E) Rok inhibition does not rescue the sprouting defect of Raf-1$^{\Delta/\Delta}$ pMECs. Y-27632 was added to the fibrin gels at indicated concentrations. Sprout formation was analyzed as in Figure 1A. Note the increased amount of individual cells scattered around the microcarrier in the f/f cultures treated with 50 μM Y-27632. A quantification of the results is shown in the right panel (minimum n = 25 microcarriers per genotype and treatment; error bars, SE of the mean). Blue traces have been added to two of the images lacking contrast to highlight the profile of the sprouts. Scale bars (B) and (C), 20 μm; (D), 10 μm; and (E), 200 μm. $p < 0.001$, according to Student's t tests. n.s., not significant.

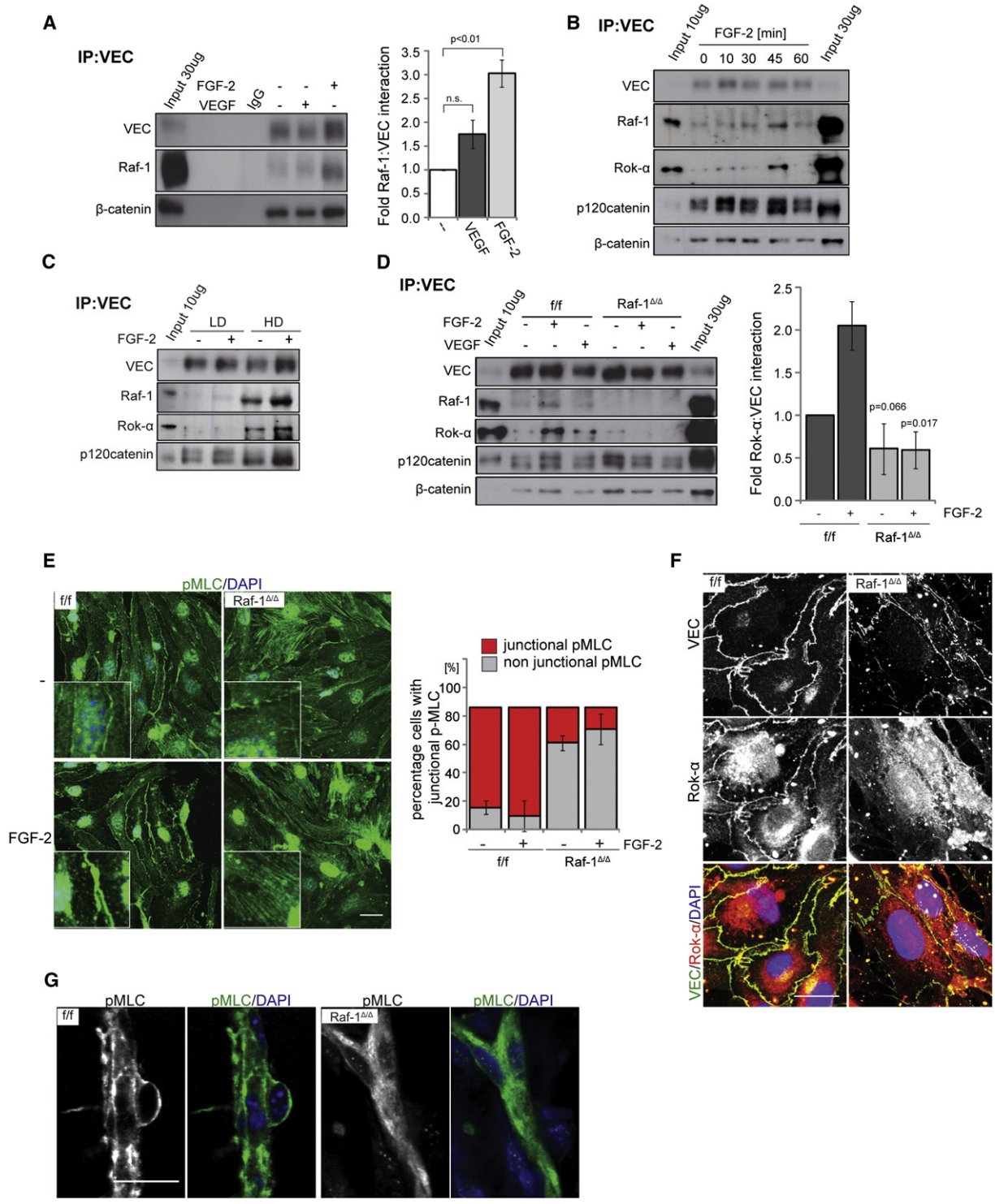

Figure 3. Raf-1 Is Required for the Recruitment of Rok-α to AJ and for Junctional Myosin Activation

(A–C) Growth factors and increasing cell densities induce the recruitment of Raf-1 and Rok-α to VEC. iMECs were treated with FGF-2 or VEGF (both 50 ng/ml) for 30 min (A) or with FGF-2 (50 ng/ml) for the indicated times (B) or seeded at low (LD) or high density (HD) (C). VEC immunoprecipitates were prepared and the presence of VEC and coimmunoprecipitating proteins was detected by immunoblotting. In (A), the right panel shows growth factor-induced recruitment of Raf-1 to VEC plotted as fold Raf-1-VEC interaction in unstimulated cells (set as 1; mean ± SE of four experiments).

(D) Raf-1 is required for growth factor-stimulated recruitment of Rok-α to VEC. iMECs were treated with FGF-2 or VEGF as in (A). The right panel shows FGF-2 induced recruitment of Rok-α to VEC plotted as fold Rok-α–VEC interaction in unstimulated cells (set as 1; mean ± SE of three experiments). The p value was calculated by comparing f/f versus Raf-1$^{\Delta/\Delta}$ cells.

required for the binding of Raf-1 to Rok-α (Niault et al., 2009), nullifies this effect (Figure 4). Thus, binding to Rok-α and to an activated G protein is essential for the function of Raf-1 in EC sprouting. With the exception of K-Ras, which contributes to the formation of Oncostatin M-induced E-cadherin cell-cell contacts in hepatocytes (Matsui et al., 2002), Ras activation is mostly associated with junction disassembly (Popoff and Geny, 2009). We show that another Ras-like G protein, Rap1, which is activated at newly formed VEC-containing cell-cell contacts (Sakurai et al., 2006; Wittchen et al., 2005) and plays an important role in the extension of nascent contacts in ECs (Figures 5 and 6) (Kooistra et al., 2005; Noda et al., 2010) and epithelial cells (Dubé et al., 2008), but is dispensable for AJ maintenance (Dubé et al., 2008; Hogan et al., 2004), is the upstream regulator of Raf-1 at AJ. Rap1 activation is necessary and sufficient to recruit Raf-1 and Rok-α to VEC, and Rap1-induced AJ maturation is blunted in Raf-1$^{\Delta/\Delta}$ iMECs (Figures 5 and 6). Unlike Ras activation in epithelial cells and in the epidermis (Ehrenreiter et al., 2009; Niault et al., 2009), Rap1 activation does not promote the association between Raf-1 and Rok-α. Collectively, therefore, the data are consistent with a model in which Rap1 activation recruits the Raf-1/Rok-α complex to VEC to locally regulate MLC2 activity and AJ dynamics during sprouting.

In contrast to Raf-1, endothelial B-Raf is not required for sprouting and does not coimmunoprecipitate with VEC under any of the conditions tested (data not shown). In good correlation with our model, Rap1 binds more efficiently to Raf-1 than to B-Raf (Hu et al., 1997; Okada et al., 1999) because of its higher affinity to the Raf-1 CRD (Okada et al., 1999). The Raf-1 CRD is also required for Rok-α binding and inhibition (Niault et al., 2009), and an exhaustive two-hybrid screen for A-Raf and Raf-1 interactors has identified the CRD as the discriminator between these two proteins (Yuryev and Wennogle, 2003). Thus, the CRD has a prominent role in conferring specificity to Raf isoforms.

EPAC and Rap1 are also crucial regulators of endothelial permeability (Cullere et al., 2005; Kooistra et al., 2005; Wittchen et al., 2005; Yan et al., 2008), and the Rap1 effector KRIT1 (CCM1; a member of the cerebral cavernous malformation family), as well as its interacting protein CCM2, are particularly important in this context (Glading et al., 2007; Stockton et al., 2010). Intriguingly, KRIT1 or CCM2-depleted cells show a dramatic increase in active RhoA and in MLC2 phosphorylation, particularly at the junctions. This correlates with the destabilization of mature junctions and with vascular leakage, which can be alleviated by treatment with a Rok inhibitor (Stockton et al., 2010). On the contrary, Raf-1$^{\Delta/\Delta}$ cells show a selective lack of MLC2 activation at nascent AJ. This correlates with defects in junction formation and sprouting, which are phenocopied by treatment of f/f cells with a Rok inhibitor or with siRNA against Rok-α (Figures 1, 2, 5, and 6). Whether the depletion of KRIT1/CCM2 has any effect on nascent AJ dynamics has not been investigated; similarly, we currently do not know whether Raf-1 ablation has an effect on endothelial permeability. However, the existence of these two pathways, impacting Rho/Rok signaling at the AJ in opposite ways, would allow for the fine regulation of AJ plasticity by EPAC/Rap1.

The control of cadherin-containing AJ by EPAC/Rap1 and myosin is not unique to ECs; epithelial cell junctions are regulated in a similar way (Dubé et al., 2008; Pannekoek et al., 2009; Papusheva and Heisenberg, 2010). Preliminary results indicate that Raf-1 is recruited to E-cadherin and regulates its distribution to the membrane in the epidermis (R.W. and M.B., unpublished data). We are currently determining whether this function of Raf-1 has an impact on epidermal barrier function.

In keratinocytes, Raf-1 inhibition of Rok-α is required for the development and maintenance of Ras-dependent tumors (Ehrenreiter et al., 2009). This is related to Rok-α's ability to promote keratinocyte differentiation by inducing EDC expression (McMullan et al., 2003) and cell cycle exit through the phosphorylation of other downstream targets, such as cofilin (Honma et al., 2006). Thus, the consequences of the interaction of Rok-α with Raf-1 are cell- and context-dependent, but their net effect is to promote tumorigenesis, either in a cell autonomous manner (inhibition of cell differentiation) or by supporting tumor-driven angiogenesis. Accordingly, approaches targeting the Raf-1/Rok-α complex may be considered attractive in the (co)therapy of cancer.

EXPERIMENTAL PROCEDURES

Matrigel Plug Assay and LLC-1 Xenografts

We subcutaneously injected 400 μl Matrigel, high concentration (BD Bioscience) supplemented with 1 μg recombinant human FGF-2 and 500 ng VEGF (R&D), or 10^6 LLC-1 cells in 100 μl PBS (Akhtar et al., 2002). Matrigel plugs were isolated 10 days postinjection and the tumors were isolated 14 days postinjection. Onset and size of tumors were monitored at least twice a week. Plugs and tumors were fixed in 4% PFA and subjected to immunohistochemical analysis. Animal experiments were authorized by the Austrian Ministry of Science and Communications, following the approval by the national Ethical Committee for Animal Experimentation.

Plasmids

Raf-1 GFP constructs were kindly provided by R.M. Lafrenie. The Raf-1 NT-CC/SS and Raf-1 NT-R89L were generated by site-directed mutagenesis (Stratagene) and verified by sequencing.

Histological Analysis

Hematoxylin/eosin staining and immunohistochemistry were performed on 3-mm-thick sections of 4% paraformaldehyde-fixed, paraffin-embedded tissue. ECs were visualized using a rat-anti-mouse-CD31 antibody (BD PharMingen) detected with the DAKO EnVision peroxidase system, followed by incubation with 0.01% diaminobenzidine (Sigma), in conjunction with avidin-biotinylated enzyme complex (Vector Laboratories) for biotinylated antibodies. Sections were counterstained with hematoxylin. A secondary

(E) pMLC is not associated with AJ in Raf-1$^{\Delta/\Delta}$ iMECs. iMECs were stimulated with FGF-2 (50 ng/ml) for 30 min. pMLC (green) and DAPI (blue) were visualized by confocal microscopy. The percentage of cells positive for junctional pMLC (mean ± SD) is shown in the lower panel.
(F) Rok-α does not colocalize with VEC in Raf-1$^{\Delta/\Delta}$ iMECs. Rok-α (red) and VEC (green) were visualized by confocal microscopy. DAPI was used as a counterstain. Scale bar: 20 μm.
(G) pMLC fails to localize at cell-cell borders in sprouts formed in matrigel plugs implanted in Raf-1$^{\Delta/\Delta EC}$ mice. Scale bar: 20 μm. In (A), IgG represents control immunoprecipitate using an unrelated, isotype-matched antibody, instead of the VEC antibody. In (A)–(D), input = whole cell lysate. See also Figure S3.

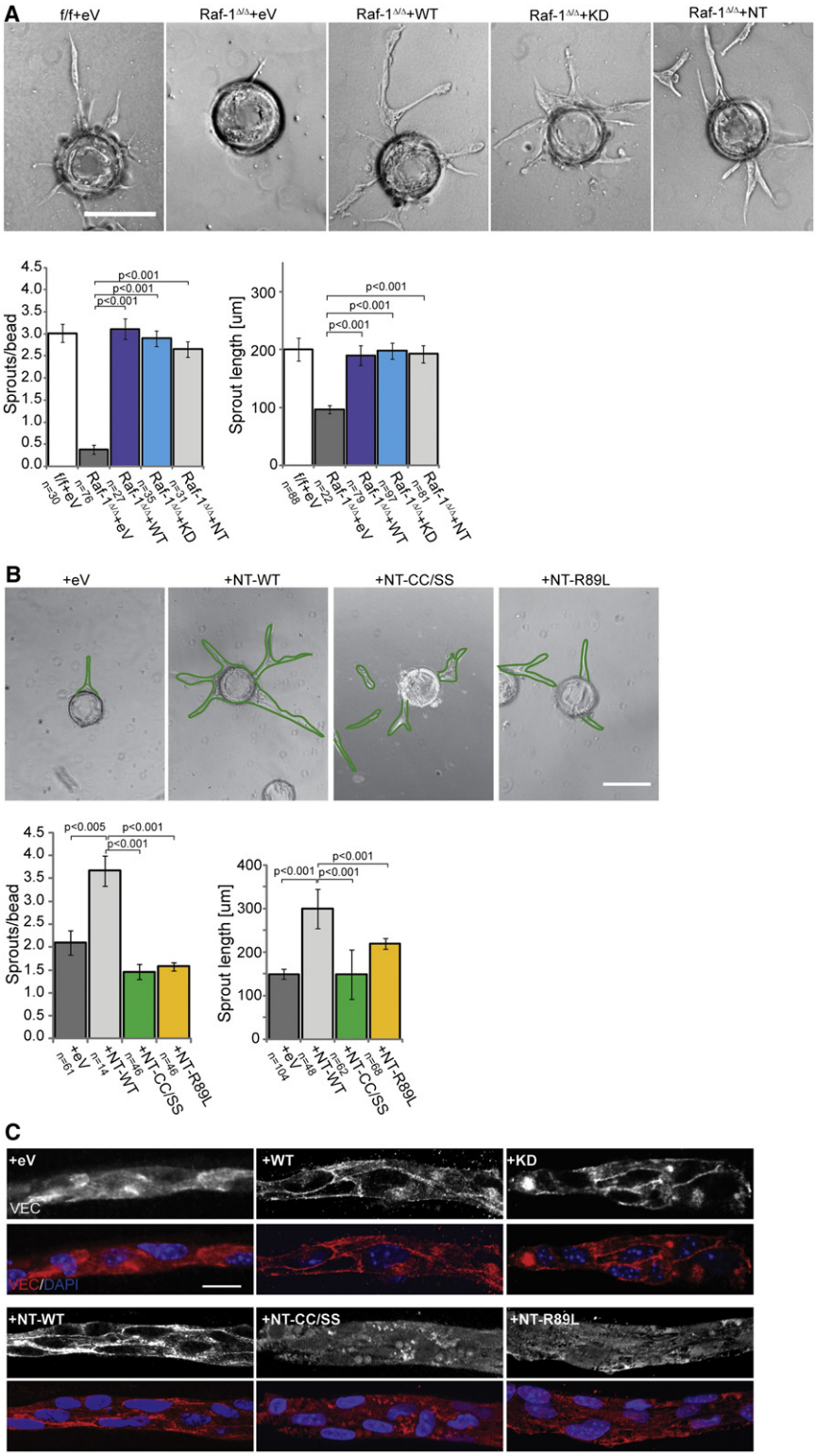

Figure 4. The N-Terminal Domain of Raf-1 Is Sufficient to Restore Sprouting and Junctional VEC in Raf-1$^{\Delta/\Delta}$ pMECs

(A) Reconstitution of Raf-1$^{\Delta/\Delta}$ pMECs with the regulatory N-terminal domain restores the number and length of sprouts formed in 3D fibrin gels.

(B) Raf-1 CRD and RBD are essential for sprouting.

(C) The N-terminal domain of Raf-1, but not the CRD and RBD mutants, restore junctional VEC in Raf-1$^{\Delta/\Delta}$ pMECs. f/f and Raf-1$^{\Delta/\Delta}$ pMECs were transfected with GFP-tagged constructs and FACS sorted. Sprouting efficiency was assessed 3 days later. The results (number of sprouts/bead and sprout length) are plotted in the lower panels (n = number of microcarriers evaluated; error bars, SE of the mean). Scale bars: (A)–(B), 200 μm; (C), 20 μm. In (B), green traces have been added to three of the images lacking contrast to highlight the profile of the sprouts.

donkey-anti-rat-Alexa594 antibody (Invitrogen) was used to visualize CD31-positive cells by immunofluorescence.

EC Isolation, Culture, Transfection/Sorting, and Immortalization

Endothelial cells were isolated using a modification of an earlier protocol (Lim and Luscinskas, 2006). Lungs were isolated from 10-day-old mice and placed in cold EC Base Medium (DMEM Medium supplemented with nonessential amino acids, 1mM sodium pyruvate [GIBCO], 25 mM HEPES pH 7.4 [Applichem], penicillin/streptomycin, and 20% FBS [Sigma]) on ice. The tissue was minced and enzymatically digested in 1 mg/ml Collagenase Type 1 (Worthington; 1 hr at 37°C). Tissue fragments were resuspended using a syringe with an 18G needle and passed through a cell strainer (70 μm mesh size; BD Falcon) to obtain a single cell suspension. Cells were seeded onto 10 cm cell culture plates (BD Falcon) coated with 2% gelatin (Sigma) and 10 μg/ml Fibronectin (Roche) and cultured in EC culture medium (EC Base + 100 μg/ml Endothelial Mitogen [Biomedical Technologies] and 100 μg/ml Heparin [Sigma]). After 48–72 hr, cells were trypsinized and incubated with rat anti-mouse ICAM-2 antibody (BD-PharMingen) coupled to dynabeads (Dynal Biotech; 1 hr at 4°C). Cell-coated beads were placed for 2 min in a magnetic particle concentrator (Dynal), washed four times with 1 ml of EC base, and seeded on 6 cm plates. The sorting was repeated once more after the cells reached confluence. The protocol reproducibly yields 95%–98% pure MECs.

pMECs were transfected with GFP-tagged Raf-1 constructs using Lipofectamine Plus (Invitrogen), in accordance with the manufacturer's protocol. Sixteen to eighteen hours after transfection, GFP$^+$ pMECs were sorted using a BD FACS Aria cell sorter, purified up to 95% GFP$^+$ cells, and left to recover overnight. Sixteen to eighteen hours later the cells were used in the fibrin gel bead assay.

Immortalized MECs (iMECs) were derived from primary ECs incubated with the supernatant of polyoma middle T antigen-producing cells (Balconi et al., 2000), supplemented with 8 μg/ml polybrene to increase infection efficiency. Infection was repeated three times at 2-day intervals.

For growth factor or 007 (Biolog) stimulation, MECs were incubated in FBS-reduced base medium (1% FBS) for 16–18 hr prior to treatment with FGF-2, VEGF, or 007 at the concentration and for the time indicated in the figure legends.

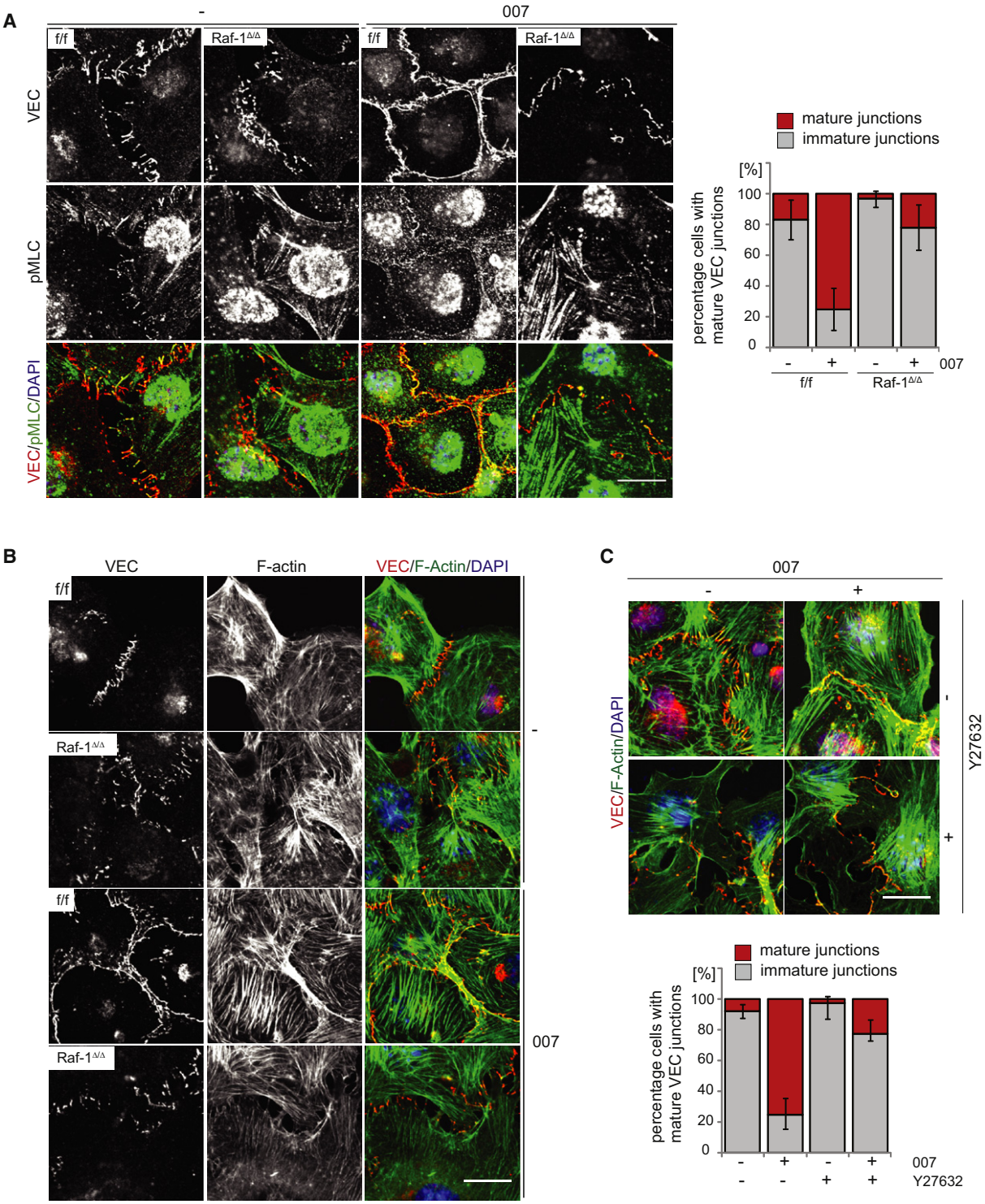

Figure 5. EPAC/Rap-Mediated AJ Maturation and Actin Bundle Formation Depends on Raf-1 and Rok-α

(A–C) iMECs were seeded on chamber slides in the presence or absence of 007 (250 μM) and of Y-27632 (20 μM). After 2 hr, the localization of VEC (red) and pMLC (green) was analyzed by confocal microscopy. DAPI (blue) was used as a counterstain. In (B)–(C), VEC (red) was used to visualize the AJ; filamentous actin (green) was visualized by phalloidin staining. Note the strong increase in AJ maturation (A) and (C) and peripheral actin bundling induced by 007 in f/f, but not in Raf-1$^{\Delta/\Delta}$ cells or in Y-27632-treated f/f cells. The graphs in (A) and (C) show the percentage of cells (mean ± SD) containing immature or mature junctions. Scale bars: 20 μm. See also Figure S3.

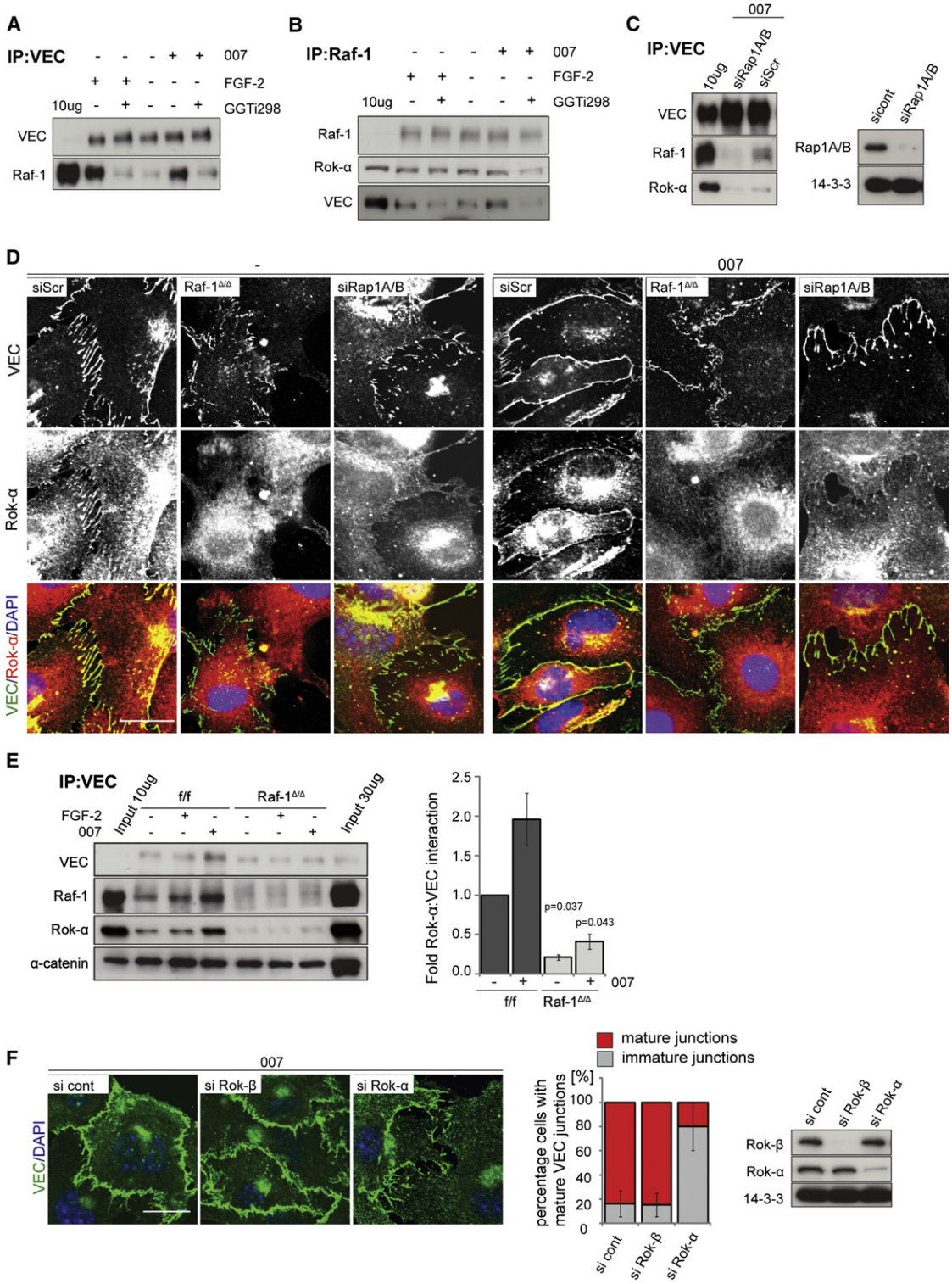

Figure 6. EPAC/Rap Activation Recruits the Raf-1/Rok-α Complex to VEC-Containing AJ

(A and B) iMECs were treated for 30 min with FGF-2 (50 ng/ml) or with the cAMP analog 007 (50 μM), a selective EPAC activator. Where indicated, cells were pretreated with GGTi-298 (10 μM; 1.5 hr) prior to stimulation to block Rap-dependent signaling. (A) VEC or (B) Raf-1 immunoprecipitates were prepared and the presence of VEC or Raf-1 and coimmunoprecipitating proteins were detected by immunoblotting.

(C) Rap1A/B is required for EPAC-mediated recruitment of Rok-α and Raf-1 to VEC. iMECS in which Rap1A and Rap1B were knocked down by siRNA interference, were stimulated with 007 (50 μM, 30 min). The presence of Rok-α and Raf-1 in VEC immunoprecipitates was detected by immunoblotting.

Gene Silencing

Rok-α (L-040429-00-0005), Rok-β (L-046504-00-0005), Rap1A (L-057058-01-0005), and Rap1B (L-062638-01-0005) were silenced using ON-TARGETplus SMARTpool siRNAs (Dharmacon). Nontargeting pool (D-001810-10-05) was used as control. In accordance with the supplier's protocol, 1×10^5 iMECs were transfected with 25 nM of the previously mentioned oligos. After 48 hr, transfection medium was changed to EC base medium. Cells were plated the next day for experiment.

Fibrin Gel Bead Assay

A previously established assay (Nakatsu et al., 2007) was optimized for pMECs. Briefly, 2,500 Cytodex beads (GE Healthcare) were incubated with 10^6 pMECs (5 hr, 37°C, and 5% CO_2) and plated overnight on a 10 cm dish to remove unattached cells. Next day, the cell-covered beads were resuspended to a concentration of ~500/ml in 2 mg/ml fibrinogen (Sigma) solution containing 0.15 U/ml aprotinin (Sigma), 200 ng/ml FGF-2, and 200 ng/ml VEGF. Aliquots were mixed with Thrombin (Sigma; 0.625 U/ml), distributed in 24-well plates (Nunc; 500 μl/well), and left to clot for 5–10 min. After further incubation (10 min, 37°C, and 5% CO_2), EC base was added to cover the clot. Sprout formation was imaged with a Zeiss Axiovert 200M equipped with an Axiocam MRm and analyzed with the Zeiss Axiovision software. For videomicroscopy, clots were imaged for 3 days every 30 min at various Z-positions using a Zeiss Axiovert 200M equipped with temperature, CO_2 and humidity control and a CoolSnap HQ2 camera. Where indicated, Rok or Rap inhibition was achieved by adding Y-27632 (Calbiochem) or GGTi298 (Calbiochem) to the fibrinogen solution.

Immunofluorescence in 3D Fibrin Gels and Whole-Mount Matrigel Plugs

For VEC staining, samples were fixed (1% PFA in 250 mM HEPES [pH 7.4], 15 min at RT), washed (TBST, 0.2% Tween-20, 15 min) prior to blocking (0.1% gelatin in PBST, 0.2% Tween, 1 hr at 4°C), and incubated with primary rat anti-mouse VEC antibodies (BD PharMingen; 1:100 in blocking solution, 1 hr at 37°C). Samples were washed thrice (30 min with PBST at RT), postfixed (4% PFA in PBS for 15 min), and washed again (30 min each TBST, PBST, blocking solution) before incubating with anti-rat-Alexa594 conjugate (1:500 overnight at 4°C). Samples were then washed (thrice with PBS and once with H_20, 30 min each) before mounting in DAKO mounting medium. Filamentous actin was detected in samples fixed in 4% PFA for 30min by staining with phalloidin-Alexa594 (Invitrogen, 1:500 in PBS, 1 hr at RT). Nuclear chromatin was stained by incubating the samples for 20–30 min in 0.5 μg/ml DAPI in PBS solution.

Immunofluorescence in 2D Cultures

Cells were permeabilized (0.2% Triton X-100 in PBS, 10 min RT), blocked (5% skim milk in PBS, 1 hr RT), and washed extensively with PBS prior to the simultaneous incubation with rat anti-mouse-VEC (BD PharMingen) and goat anti-mouse-pMLC (Santa Cruz) antibodies (1:100 in 3% BSA, overnight at 4°C). After thorough washing in PBS, cells were stained with the appropriate secondary antibody (anti-rat-Alexa594, anti-goat-Alexa488, Invitrogen; 1:500 in 5% skim milk, 1 hr at RT), washed in PBS, counterstained with DAPI, and mounted in DAKO fluorescent mounting medium. The results of the immunofluorescence experiments were quantified by analyzing at least 100 cells/sample from two independent experiments and are plotted in the figures as mean ± SD.

Immunoprecipitation and Immunoblotting

Cells were washed once with ice-cold PBS and lysed in IP-buffer (20 mM Tris/acetate [pH7.0], 0.27 M sucrose, 1% Triton X-100, 1 mM DTT, 1 mM EGTA, 1 mM EDTA, 1 mM Na_3VO_4, 25 m MNaF, 1 mM PMSF, and protease inhibitor cocktail [Roche]). We precleared 500 μg clear cell lysate (1 μg protein/μl) with 40 μl ProteinG-Sepharose beads (Pierce, 1 hr at 4°C) and incubated with the relevant antibodies (rat anti-mouse-VEC 1:100, rabbit anti-mouse Raf-1, Cell Signaling; 1:100 overnight at 4°C). Immunocomplexes were collected by adding 40 μl protein G-sepharose beads (1 hr at 4°C).

For immunoblotting, cell lysates and immunoprecipitates were subjected to SDS-PAGE and blotted to nitrocellulose membranes subsequently probed with α-actin, α-14-3-3 α-pMYPT1, α-Rok-α, and α-pCofilin (Santa Cruz); α-Raf-1, α-α-catenin, α-β-catenin, and α-p120catenin (BD Transduction Laboratories); α-VEC (BD PharMingen); and α-pMLC2 and α-pERK (Cell Signaling). After incubation with the appropriate secondary antibody, the antigens were visualized by ECL (Pierce).

Statistical Analysis

p values were calculated with the two-tailed Student's t test. $p \leq 0.05$ is considered statistically significant.

SUPPLEMENTAL INFORMATION

Supplemental information includes fives figures, Supplemental Experimental Procedures, and two movies and can be found with this article online at doi:10.1016/j.devcel.2011.11.012.

ACKNOWLEDGMENTS

We thank F. Propst and H. Bos for helpful discussions; K. Aumayr (IMP, Vienna), T. Sauer, C. Bogner, M. Ehlers, and the animal house team for excellent technical assistance; A. Varga for help with site-directed mutagenesis; and B. Arnold for the *Tie2-Cre* mice (DKFZ, Heidelberg). This work was supported by AICR grant 06-0572 and by Austrian Research Fund grant SFB021 (to M.B.).

Received: January 27, 2011
Revised: November 9, 2011
Accepted: November 28, 2011
Published online: December 29, 2011

REFERENCES

Abraham, S., Yeo, M., Montero-Balaguer, M., Paterson, H., Dejana, E., Marshall, C.J., and Mavria, G. (2009). VE-Cadherin-mediated cell-cell interaction suppresses sprouting via signaling to MLC2 phosphorylation. Curr. Biol. *19*, 668–674.

Akhtar, N., Dickerson, E.B., and Auerbach, R. (2002). The sponge/Matrigel angiogenesis assay. Angiogenesis *5*, 75–80.

Alavi, A., Hood, J.D., Frausto, R., Stupack, D.G., and Cheresh, D.A. (2003). Role of Raf in vascular protection from distinct apoptotic stimuli. Science *301*, 94–96.

Alavi, A.S., Acevedo, L., Min, W., and Cheresh, D.A. (2007). Chemoresistance of endothelial cells induced by basic fibroblast growth factor depends on Raf-1-mediated inhibition of the proapoptotic kinase, ASK1. Cancer Res. *67*, 2766–2772.

Baccarini, M. (2005). Second nature: biological functions of the Raf-1 "kinase". FEBS Lett. *579*, 3271–3277.

Balconi, G., Spagnuolo, R., and Dejana, E. (2000). Development of endothelial cell lines from embryonic stem cells: A tool for studying genetically manipulated endothelial cells in vitro. Arterioscler. Thromb. Vasc. Biol. *20*, 1443–1451.

(D) Raf-1 and Rap1 are required for efficient Rok-α recruitment to VEC junctions. iMECs in which Rap1A and Rap1B were knocked down by siRNA interference, were seeded for 2 hr in the presence or absence of 007 (250 μM). Rok-α (red) and VEC (green) were visualized by confocal microscopy. DAPI (blue) was used as a counterstain. Note the absence of junctional Rok-α in Raf-$1^{\Delta/\Delta}$ cells and in f/f cells treated with GGTi298.
(E) iMECs were treated and VEC immunoprecipitates were analyzed as in (A). In the right panel, 007-induced recruitment of Rok-α to VEC is plotted as fold Rok-α-VEC interaction in unstimulated cells (set as 1; mean ± SE of three experiments). The *p* value was calculated comparing f/f versus Raf-$1^{\Delta/\Delta}$ cells.
(F) Small interfering RNA (siRNA)-mediated knock down of Rok-α, but not Rok-β abrogates 007-induced AJ maturation. siRNA-treated cells were plated for 2 hr in the presence of 007 (250 μM). VEC (green) and nuclei (DAPI, blue) were visualized by confocal microscopy. The graph shows the percentage of cells with mature AJ (mean ± SD). Knockdown efficiency is shown by immunoblotting. Scale bars: 20 μm. See also Figures S4 and S5.

Carmona, G., Göttig, S., Orlandi, A., Scheele, J., Bäuerle, T., Jugold, M., Kiessling, F., Henschler, R., Zeiher, A.M., Dimmeler, S., and Chavakis, E. (2009). Role of the small GTPase Rap1 for integrin activity regulation in endothelial cells and angiogenesis. Blood *113*, 488–497.

Cascone, I., Giraudo, E., Caccavari, F., Napione, L., Bertotti, E., Collard, J.G., Serini, G., and Bussolino, F. (2003). Temporal and spatial modulation of Rho GTPases during in vitro formation of capillary vascular network. Adherens junctions and myosin light chain as targets of Rac1 and RhoA. J. Biol. Chem. *278*, 50702–50713.

Chrzanowska-Wodnicka, M., Kraus, A.E., Gale, D., White, G.C., 2nd, and Vansluys, J. (2008). Defective angiogenesis, endothelial migration, proliferation, and MAPK signaling in Rap1b-deficient mice. Blood *111*, 2647–2656.

Chung, A.S., Lee, J., and Ferrara, N. (2010). Targeting the tumour vasculature: insights from physiological angiogenesis. Nat. Rev. Cancer *10*, 505–514.

Cullere, X., Shaw, S.K., Andersson, L., Hirahashi, J., Luscinskas, F.W., and Mayadas, T.N. (2005). Regulation of vascular endothelial barrier function by Epac, a cAMP-activated exchange factor for Rap GTPase. Blood *105*, 1950–1955.

Dejana, E., Tournier-Lasserve, E., and Weinstein, B.M. (2009). The control of vascular integrity by endothelial cell junctions: molecular basis and pathological implications. Dev. Cell *16*, 209–221.

Dubé, N., Kooistra, M.R., Pannekoek, W.J., Vliem, M.J., Oorschot, V., Klumperman, J., Rehmann, H., and Bos, J.L. (2008). The RapGEF PDZ-GEF2 is required for maturation of cell-cell junctions. Cell. Signal. *20*, 1608–1615.

Dudek, S.M., and Garcia, J.G. (2001). Cytoskeletal regulation of pulmonary vascular permeability. J. Appl. Physiol. *91*, 1487–1500.

Ehrenreiter, K., Piazzolla, D., Velamoor, V., Sobczak, I., Small, J.V., Takeda, J., Leung, T., and Baccarini, M. (2005). Raf-1 regulates Rho signaling and cell migration. J. Cell Biol. *168*, 955–964.

Ehrenreiter, K., Kern, F., Velamoor, V., Meissl, K., Galabova-Kovacs, G., Sibilia, M., and Baccarini, M. (2009). Raf-1 addiction in Ras-induced skin carcinogenesis. Cancer Cell *16*, 149–160.

Eilken, H.M., and Adams, R.H. (2010). Dynamics of endothelial cell behavior in sprouting angiogenesis. Curr. Opin. Cell Biol. *22*, 617–625.

Enserink, J.M., Christensen, A.E., de Rooij, J., van Triest, M., Schwede, F., Genieser, H.G., Døskeland, S.O., Blank, J.L., and Bos, J.L. (2002). A novel Epac-specific cAMP analogue demonstrates independent regulation of Rap1 and ERK. Nat. Cell Biol. *4*, 901–906.

Fischer, R.S., Gardel, M., Ma, X., Adelstein, R.S., and Waterman, C.M. (2009). Local cortical tension by myosin II guides 3D endothelial cell branching. Curr. Biol. *19*, 260–265.

Forde, A., Constien, R., Gröne, H.J., Hämmerling, G., and Arnold, B. (2002). Temporal Cre-mediated recombination exclusively in endothelial cells using Tie2 regulatory elements. Genesis *33*, 191–197.

Gavard, J., and Gutkind, J.S. (2006). VEGF controls endothelial-cell permeability by promoting the beta-arrestin-dependent endocytosis of VE-cadherin. Nat. Cell Biol. *8*, 1223–1234.

Glading, A., Han, J., Stockton, R.A., and Ginsberg, M.H. (2007). KRIT-1/CCM1 is a Rap1 effector that regulates endothelial cell cell junctions. J. Cell Biol. *179*, 247–254.

Grazia Lampugnani, M., Zanetti, A., Corada, M., Takahashi, T., Balconi, G., Breviario, F., Orsenigo, F., Cattelino, A., Kemler, R., Daniel, T.O., and Dejana, E. (2003). Contact inhibition of VEGF-induced proliferation requires vascular endothelial cadherin, beta-catenin, and the phosphatase DEP-1/CD148. J. Cell Biol. *161*, 793–804.

Herrmann, C., Horn, G., Spaargaren, M., and Wittinghofer, A. (1996). Differential interaction of the ras family GTP-binding proteins H-Ras, Rap1A, and R-Ras with the putative effector molecules Raf kinase and Ral-guanine nucleotide exchange factor. J. Biol. Chem. *271*, 6794–6800.

Hoang, M.V., Whelan, M.C., and Senger, D.R. (2004). Rho activity critically and selectively regulates endothelial cell organization during angiogenesis. Proc. Natl. Acad. Sci. USA *101*, 1874–1879.

Hogan, C., Serpente, N., Cogram, P., Hosking, C.R., Bialucha, C.U., Feller, S.M., Braga, V.M., Birchmeier, W., and Fujita, Y. (2004). Rap1 regulates the formation of E-cadherin-based cell-cell contacts. Mol. Cell. Biol. *24*, 6690–6700.

Honma, M., Benitah, S.A., and Watt, F.M. (2006). Role of LIM kinases in normal and psoriatic human epidermis. Mol. Biol. Cell *17*, 1888–1896.

Hood, J.D., Bednarski, M., Frausto, R., Guccione, S., Reisfeld, R.A., Xiang, R., and Cheresh, D.A. (2002). Tumor regression by targeted gene delivery to the neovasculature. Science *296*, 2404–2407.

Hu, C.D., Kariya, K., Kotani, G., Shirouzu, M., Yokoyama, S., and Kataoka, T. (1997). Coassociation of Rap1A and Ha-Ras with Raf-1 N-terminal region interferes with ras-dependent activation of Raf-1. J. Biol. Chem. *272*, 11702–11705.

Jesenberger, V., Procyk, K.J., Rüth, J., Schreiber, M., Theussl, H.C., Wagner, E.F., and Baccarini, M. (2001). Protective role of Raf-1 in Salmonella-induced macrophage apoptosis. J. Exp. Med. *193*, 353–364.

Kooistra, M.R., Corada, M., Dejana, E., and Bos, J.L. (2005). Epac1 regulates integrity of endothelial cell junctions through VE-cadherin. FEBS Lett. *579*, 4966–4972.

Kooistra, M.R., Dubé, N., and Bos, J.L. (2007). Rap1: a key regulator in cell-cell junction formation. J. Cell Sci. *120*, 17–22.

Lampugnani, M.G., Orsenigo, F., Gagliani, M.C., Tacchetti, C., and Dejana, E. (2006). Vascular endothelial cadherin controls VEGFR-2 internalization and signaling from intracellular compartments. J. Cell Biol. *174*, 593–604.

Lim, Y.C., and Luscinskas, F.W. (2006). Isolation and culture of murine heart and lung endothelial cells for in vitro model systems. Methods Mol. Biol. *341*, 141–154.

Liu, Z., Tan, J.L., Cohen, D.M., Yang, M.T., Sniadecki, N.J., Ruiz, S.A., Nelson, C.M., and Chen, C.S. (2010). Mechanical tugging force regulates the size of cell-cell junctions. Proc. Natl. Acad. Sci. USA *107*, 9944–9949.

Matsui, T., Kinoshita, T., Morikawa, Y., Tohya, K., Katsuki, M., Ito, Y., Kamiya, A., and Miyajima, A. (2002). K-Ras mediates cytokine-induced formation of E-cadherin-based adherens junctions during liver development. EMBO J. *21*, 1021–1030.

McMullan, R., Lax, S., Robertson, V.H., Radford, D.J., Broad, S., Watt, F.M., Rowles, A., Croft, D.R., Olson, M.F., and Hotchin, N.A. (2003). Keratinocyte differentiation is regulated by the Rho and ROCK signaling pathway. Curr. Biol. *13*, 2185–2189.

Mikula, M., Schreiber, M., Husak, Z., Kucerova, L., Rüth, J., Wieser, R., Zatloukal, K., Beug, H., Wagner, E.F., and Baccarini, M. (2001). Embryonic lethality and fetal liver apoptosis in mice lacking the c-raf-1 gene. EMBO J. *20*, 1952–1962.

Nakatsu, M.N., Davis, J., and Hughes, C.C. (2007). Optimized fibrin gel bead assay for the study of angiogenesis. J. Vis. Exp. *3*, 186.

Nassar, N., Horn, G., Herrmann, C., Scherer, A., McCormick, F., and Wittinghofer, A. (1995). The 2.2 A crystal structure of the Ras-binding domain of the serine/threonine kinase c-Raf1 in complex with Rap1A and a GTP analogue. Nature *375*, 554–560.

Nassar, N., Horn, G., Herrmann, C., Block, C., Janknecht, R., and Wittinghofer, A. (1996). Ras/Rap effector specificity determined by charge reversal. Nat. Struct. Biol. *3*, 723–729.

Niault, T., Sobczak, I., Meissl, K., Weitsman, G., Piazzolla, D., Maurer, G., Kern, F., Ehrenreiter, K., Hamerl, M., Moarefi, I., et al. (2009). From autoinhibition to inhibition in trans: the Raf-1 regulatory domain inhibits Rok-alpha kinase activity. J. Cell Biol. *187*, 335–342.

Noda, K., Zhang, J., Fukuhara, S., Kunimoto, S., Yoshimura, M., and Mochizuki, N. (2010). Vascular endothelial-cadherin stabilizes at cell-cell junctions by anchoring to circumferential actin bundles through alpha- and beta-catenins in cyclic AMP-Epac-Rap1 signal-activated endothelial cells. Mol. Biol. Cell *21*, 584–596.

Okada, T., Hu, C.D., Jin, T.G., Kariya, K., Yamawaki-Kataoka, Y., and Kataoka, T. (1999). The strength of interaction at the Raf cysteine-rich domain is a critical determinant of response of Raf to Ras family small GTPases. Mol. Cell. Biol. *19*, 6057–6064.

Pannekoek, W.J., Kooistra, M.R., Zwartkruis, F.J., and Bos, J.L. (2009). Cell-cell junction formation: the role of Rap1 and Rap1 guanine nucleotide exchange factors. Biochim. Biophys. Acta *1788*, 790–796.

Papusheva, E., and Heisenberg, C.-P. (2010). Spatial organization of adhesion: force-dependent regulation and function in tissue morphogenesis. EMBO J. *29*, 2753–2768.

Piazzolla, D., Meissl, K., Kucerova, L., Rubiolo, C., and Baccarini, M. (2005). Raf-1 sets the threshold of Fas sensitivity by modulating Rok-alpha signaling. J. Cell Biol. *171*, 1013–1022.

Popoff, M.R., and Geny, B. (2009). Multifaceted role of Rho, Rac, Cdc42 and Ras in intercellular junctions, lessons from toxins. Biochim. Biophys. Acta *1788*, 797–812.

Qian, Y., Vogt, A., Vasudevan, A., Sebti, S.M., and Hamilton, A.D. (1998). Selective inhibition of type-I geranylgeranyltransferase in vitro and in whole cells by CAAL peptidomimetics. Bioorg. Med. Chem. *6*, 293–299.

Rolfe, B.E., Worth, N.F., World, C.J., Campbell, J.H., and Campbell, G.R. (2005). Rho and vascular disease. Atherosclerosis *183*, 1–16.

Sakurai, A., Fukuhara, S., Yamagishi, A., Sako, K., Kamioka, Y., Masuda, M., Nakaoka, Y., and Mochizuki, N. (2006). MAGI-1 is required for Rap1 activation upon cell-cell contact and for enhancement of vascular endothelial cadherin-mediated cell adhesion. Mol. Biol. Cell *17*, 966–976.

Stockton, R.A., Shenkar, R., Awad, I.A., and Ginsberg, M.H. (2010). Cerebral cavernous malformations proteins inhibit Rho kinase to stabilize vascular integrity. J. Exp. Med. *207*, 881–896.

Wittchen, E.S., Worthylake, R.A., Kelly, P., Casey, P.J., Quilliam, L.A., and Burridge, K. (2005). Rap1 GTPase inhibits leukocyte transmigration by promoting endothelial barrier function. J. Biol. Chem. *280*, 11675–11682.

Yamada, S., and Nelson, W.J. (2007). Localized zones of Rho and Rac activities drive initiation and expansion of epithelial cell-cell adhesion. J. Cell Biol. *178*, 517–527.

Yan, J., Li, F., Ingram, D.A., and Quilliam, L.A. (2008). Rap1a is a key regulator of fibroblast growth factor 2-induced angiogenesis and together with Rap1b controls human endothelial cell functions. Mol. Cell. Biol. *28*, 5803–5810.

Yuryev, A., and Wennogle, L.P. (2003). Novel raf kinase protein-protein interactions found by an exhaustive yeast two-hybrid analysis. Genomics *81*, 112–125.